

# Measurement and Analysis of Banding Artifacts in Color Electrophotographic Printers

Thanh H. Ha and Jan P. Allebach, Purdue University, West Lafayette, Indiana, USA; and Douksoon Cha, Samsung Electronics Co., LTD., Suwon, Korea.

## Abstract

We introduce a new banding analysis system which contains a banding measurement tool and a spatial-visualization tool. The banding measurement tool is based on image analysis to measure color banding exhibited by color laser printers. The tool analyzes a specially designed test page and provides the principal banding frequency components from both the primary and secondary colorant planes. On the other hand, the spatial-visualization tool is intended to help the users better understand from a qualitative perspective the appearance of the color banding on their printed test pages. The overall banding analysis system is very useful for engineers in printer industry to investigate banding in color laser printers throughout all stages of the printer development life cycle.

## Introduction

Banding is one of the most undesirable print artifacts that limits print quality in the electrophotographic (EP) and inkjet (IJ) printer technologies. Banding is perceived by the human visual system as achromatic variations (with monochrome printers), or both achromatic and chromatic variations (with color printers) in the paper process direction. With EP (i.e. laser) printers, banding results from non-uniform line spacing which is primarily caused by fluctuations in angular velocity of the optical photoconductor (OPC) drum.

Because of the negative effects of banding on printer quality, there has been considerable research devoted to reducing banding [1-4]. Throughout the stages of the printer development life cycle, it is necessary that printer engineers can frequently measure the principal banding frequencies exhibited by their developing printer prototypes, and based on this information, modify the printer design to reduce the banding artifacts. Lin et al [4] developed an image-analysis-based method which analyzes a specially designed test page to characterize banding exhibited by monochrome laser printers. Ali [5] developed a banding analysis tool for monochrome banding measurement which uses the same method developed by Lin. Ali's tool has capabilities to deal with various practical issues that affect the banding measurement accuracy such as nonlinear scanner tone reproduction, scanner modulation transfer function (MTF), spatial distortions, and low contrast of printed test pages. However, as far as we know, no such tool has been reported in the literature for measuring the banding exhibited by color laser printers. The study of color banding is complicated because the color banding signal is physically defined in a 3-D color space, while banding perception is described in an 1-D sense as more or less banding [6]. Furthermore, how banding from individual colorant planes interacts to produce the overall color banding signal is still not clearly known.

In this paper, we introduce a new banding analysis system which includes a banding measurement tool and a spatial-visualization tool. The banding measurement tool is based on an image analysis approach to measure banding frequencies exhibited by color laser printers. The tool analyzes a specially designed test page and provides the principal banding frequency components from both primary and secondary colorant planes. The spatial-visualization tool, on the other hand, is intended to help printer engineers better understand from a qualitative perspective the appearance of color banding in their printed test pages. Our banding analysis system is for characterization from a colorimetric viewpoint of color banding as printed on the pages. There are no psychophysical experiments involved in the measurement.

In this research, we measure banding from two sources: the variations of scan line spacing of each primary colorant, and the process-direction variations of the observed primary and secondary colorants on the printed pages. We call the signals from the former the "mechanical banding" (MB) and those from the latter the "visual banding" (VB). While MB reflects only the contributions of fluctuations in the angular velocity of the OPC drum to banding, VB reflects all contributions of the entire printing process to banding, such as fluctuations in the angular velocity of the OPC drum, the developer rollers, the fuser rollers, etc. VB also reflects the possible suppression of the impact of upstream fluctuations by downstream behaviors of the printing process, including the interaction of colorant media with light on the printed pages.

The remainder of the paper is organized as follows: In the next section, we will describe our specially designed test page. Then, we will discuss our scanner calibration method and the distortion correction module. Next, we will discuss the MB pattern analysis, VB pattern analysis, and the spatial visualization of the measured VB signals. After that, we will present our banding measurement results for a specific color laser printer. The final section contains the conclusions about our study. In this paper, for the sake of simplicity, we will use the notation CIE Lab to refer to CIE 1976  $L^*a^*b^*$  (with  $2^\circ$  observer and D65 illumination). We also assume throughout this paper that the horizontal and vertical directions are, respectively, the scan and process directions for the printer.

## Test Page Design

Our test page contains two types of banding patterns: the mechanical banding (MB) pattern and the visual banding (VB) pattern that form the basis for banding signal capture.

**MB pattern:** This type of pattern is designed to capture the MB signals from the primary colorant planes (cyan, magenta, and yellow). Figure 1(a) shows a crop from the top of a printed magenta MB pattern. An MB pattern of a primary colorant consists

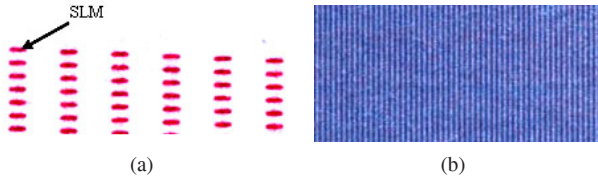


**Figure 1.** (a) A crop from the top of a printed magenta MB pattern; (b) A crop from a printed blue VB pattern.

of six columns of scan line marks (SLMs). Each SLM is designed to establish the position of one scan line of the corresponding colorant plane. These SLMs are offset in a multi-column format to permit the segmentation of the individual SLMs, and to eliminate the interaction between the exposures of the marks on the adjacent lines. For each primary colorant, we place two symmetrical MB patterns on either side of the test page to compensate for the effect of skew.

**VB pattern:** This type of pattern is designed to capture the VB signals from both the primary and secondary (red, green, and blue) colorant planes. Figure 1(b) shows a crop from a printed blue VB pattern. A VB pattern is a mid-tone fill patch generated by finely spacing vertical lines of the solid corresponding color. By using vertical line fill patterns instead of halftone fill patterns, we can eliminate the effect of the halftone on the banding analysis results. Taking into account the instability of laser printers, especially the dot gain effect, we place one vertical solid color line at every fourth column of addressable pixels to generate a mid-tone fill VB pattern that when printed will exhibit the most visible banding.

Besides the MB and VB patterns, we design three 32-pixel-wide vertical lines of solid primary colors on the test page to capture the extreme values of the corresponding primary colorants. There are also two identical black vertical lines on the page, along each of which we space eight horizontal black registration marks. These registration marks will be used to determine the locations of the control points for the distortion correction module.

## Color Scanner Calibration

Because scanners typically are not colorimetric devices, to use a desktop scanner as a measurement device, we need to calibrate it carefully. We employ the model-based method found in [7] for our scanner calibration process. This method consists of two steps: gray balancing curve fitting and transformation matrix computation.

In the first step, we use the 24 gray patches of a Kodak Q-60<sup>1</sup> target as the stimuli. The Gain-Gamma-Offset (GGO) model found in [5] is used to fit three separate gray balancing curves for three color channels (R, G, and B). In the second step, we use linear regression to compute the transformation matrices. Since scanners typically do not span the subspace of the human visual system, to increase the calibration accuracy, we compute different transformation matrices for colors that span different directions in the color cube (Fig. 2), corresponding to the different colorant combinations that occur in the MB and VB patterns.

To generate a training set for colors spanning from white to a primary color vertex, we start with a uniform patch of 100%

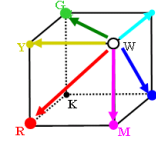


**Figure 2.** The color cube with different color directions.

density level of the corresponding color. We then use the native halftone of the target printer to gradually lighten this default patch, eventually obtaining a large training set of different density levels.

The distributions of toner particles in the secondary colorant patterns are more complicated. Let's take the blue VB pattern as an example. When examining a scanned blue VB pattern at sufficient magnification to observe individual pixels in the scanned image, we see many different pixel values that span a considerable portion of the CMYK color cube, including pixels that look like cyan, pixels that look like magenta, pixels that look like blue, pixels that look like white, and everything in between. For each secondary colorant, we use the VB pattern which is the same as the VB pattern on the test page as the basis for generating the training set. We then use a direct binary search (DBS) screen [8] to lighten this pattern in a spatially homogeneous manner. In this way, we generate a large set of different distributions of toner particles that are similar to those that we observe with the normally printed VB pattern. The native halftone of the printer is not a good choice for this since it will generate periodically repeated arrangement of colorant dots that microscopically exhibit a much smaller set of colorant combinations.

The testing sets are generated in the same way as the training sets, but with different density levels. Using this calibration method for an Epson Perfection 4870<sup>2</sup> scanning at 600 dpi and with 24-bit output, we obtain average testing errors in  $\Delta E$  units for the three primary colorants: cyan, magenta, and yellow, as 0.87, 1.56, and 1.61, respectively. Also, the average testing errors in  $\Delta E$  units for the three secondary colorants: red, green, and blue are 1.06, 1.84, and 0.95, respectively.

## Distortion Correction

Scanned test pages often have some spatial distortions (skewing, shearing, translation, etc.) which will negatively affect the accuracy of our banding analyses. To compensate for these distortions, we apply a local quadrilateral-transformation-based method to the scanned test page image.

As described in the "Test Page Design" section, along each vertical black line on the test page, we placed eight equally spaced horizontal registration marks. The centroids of these registration marks will serve as the control points in the quadrilateral transformation. We first initialize a white image with the same size as the designed test page image and with the known locations of the designed control points. We also detect the corresponding control points on the scanned test page. Then we apply the distortion correction module separately to each quadrilateral region of scanned data defined by four registration marks to obtain a corrected version. The distortion correction module consists of two steps. In

<sup>1</sup>Eastman Kodak Company, 343 State St., Rochester, NY, 14650.

<sup>2</sup>Epson, 3840 Kilroy Airport Way, Long Beach, CA 90806.

step 1, for each point on the corrected image, based on the locations of the control points on the corrected image and those bounding the scanned region that is currently being processed, we take the quadrilateral transformation to find a corresponding point on the distorted image. In step 2, we fill each point on the corrected image with the color of its corresponding point on the distorted image. In the case that the spatial coordinates of a corresponding point on the distorted image are not integers, interpolation is used to estimate color values of that point.

## MB Analysis

The MB patterns are designed to capture the variations of the scan line spacing for the three primary colorants. To analyze an MB pattern of a primary colorant, we first segment this pattern from the scanned test page. In order to provide good discrimination between the SLMs and the background media on which they are printed and to fully utilize the information in the RGB signal, we convert the scanned MB patterns to CIE Lab and convert the image data to gray-scale in terms of  $\Delta E$  units from the respective solid colorant. Next, we segment every individual SLM in this gray-scale image, compute the vertical distances between successive SLMs, and subtract the mean distance from these distances to obtain a variation sequence. In the absence of mechanical banding, the elements of this sequence would all be zero. With mechanical banding, we observe quasi-periodic fluctuations in this sequence that may lead to banding artifacts. The spectra computed by taking the discrete Fourier transform of this sequence will reveal the principal components of the mechanical banding. The mechanical banding spectra are normalized such that a pure sinusoid with amplitude 1/600 inch (in the case that the test page is printed at 600 dpi) will correspond to an FFT magnitude of unity.

Let's consider in more detail the technique we use to convert an MB pattern, initially in scanner RGB space, to a gray-scale image in  $\Delta E$  units from the respective solid colorant. When we plot the color data of a MB pattern in the CIE Lab space, we observe that these color points distribute in a certain direction from an extreme point corresponding to the respective solid colorant to another extreme point corresponding to paper white (Fig. 3(a)). We employ the method found in [7] to fit the data to this line. Two extreme points  $A$  and  $B$  of the line are computed by averaging two vertical strips of the paper white and solid primary colorant, respectively. The equations below show how to compute the scalar-valued signal in  $\Delta E$  units from a solid primary colorant for color point  $Q$  illustrated in Fig. 3(b).

$$s_Q = \begin{cases} \left\| \vec{OB} - \vec{OA} \right\| & \text{if } \left\| \vec{AQ'} \right\| \geq \left\| \vec{OB} - \vec{OA} \right\| \\ 0 & \text{if } \left\| \vec{AQ'} \right\| \leq 0 \\ \left\| \vec{AQ'} \right\| & \text{otherwise,} \end{cases} \quad (1)$$

where  $Q$  is a color point,  $O$  is the origin of the CIE Lab space,  $Q'$  is the projected point of  $Q$  on the line  $\vec{AB}$ , and  $\|\bullet\|$  is the Euclidean-norm operator.

## VB Analysis

For each colorant (either a primary or a secondary colorant), we analyze its printed VB pattern to measure the process-direction

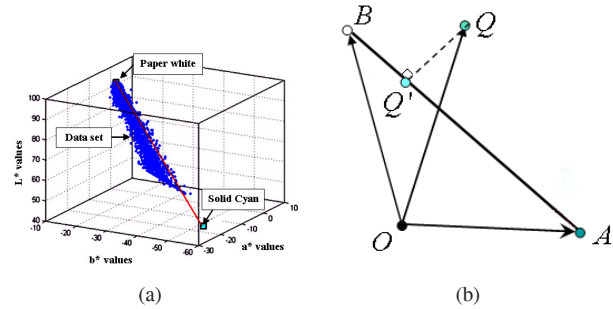


**Figure 3.** (a) The color distribution of cyan MB data in CIE Lab space; (b) A color point  $Q$  of that color data and the line determined by connecting two extreme points  $A$  and  $B$ .

variations of the observed primary and secondary colorants on the printed test page. We first convert this VB pattern from scanner RGB to linear RGB, then take horizontal projection to obtain a projected profile in linear RGB. Next, we transform this profile from linear RGB to CIE XYZ, and then to CIE Lab space. Plotting the projected profile in CIE Lab space, we also observe that the profile data distributes as a cloud along a certain direction which is determined using Principal Component Analysis (PCA). We extract the visual banding signal by computing the color differences in  $\Delta E$  units between the projected points of the color data on this line and the color mean.

Additionally, we compute in hue, chrominance, and luminance the fluctuations of the projected profile around the mean value. The spectra obtained by taking the discrete Fourier transform of these fluctuation sequences will reveal the strength of the principal components of banding in the corresponding color attributes. The visual banding spectrum in either  $\Delta E$ ,  $\Delta L$ , or  $\Delta c$  units is normalized such that a pure sinusoid with amplitude of one unit will correspond to an FFT magnitude of unity. Similarly, the visual banding spectrum in  $\Delta h$  units is normalized such that a pure sinusoid with amplitude of one degree will yield an FFT magnitude of unity.

## Spatial Visualization of Visual Banding

The purpose of the spatial visualization tool is to provide a capability to help engineers better understand from a qualitative perspective the appearance of color banding in their printed test pages. The tool is intended to achieve this by separating out the different signal components that govern the appearance of color and allowing the user to vary the strength of each component. We generate the visual representations of the color banding based on the visual banding signals that we extract from the VB patterns, as discussed in the preceding section.

## Banding Analysis Results

In this section, we present our banding analysis results for a particular color EP printer. We first print the test page with this printer at 600 dpi using a direct print mode provided by the manufacturer. This mode allows us to directly access the CMYK channels of the printer to prevent any undesirable colorants from being printed as a result of color table conversions. After that, we scan the print-out with an Epson Perfection 4870 scanner which has been calibrated using the method described in this paper. The

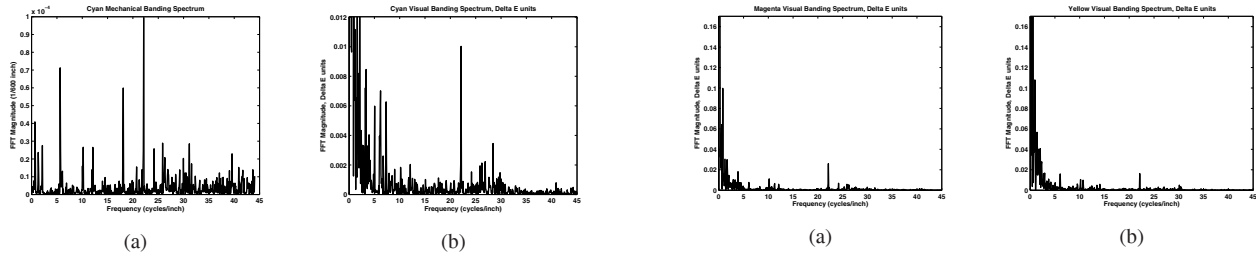


**Figure 4.** (a) Cyan mechanical banding spectrum in the range 0-45 cycles/inch; (b) Cyan visual banding spectrum in the range 0-45 cycles/inch.

banding measurement tool then analyzes the scanned test page and finally provides a variety of output banding spectra.

Because our test printer has only one OPC drum shared by all four primary colorant planes, we obtain very similar mechanical banding spectra for the three primary colorants included in our test. Figure 4(a) shows the cyan mechanical banding spectrum in the range from 0 to 45 cycles/inch. We see that the mechanical banding spectrum for cyan has principal frequencies at 0.7, 1.5, 2, 5.5, 10, 12, 18, 22, 24, 26, 28.5, 32, and 39 cycles/inch, among which the peak located at 22 cycles/inch is dominant.

We also observe the similarity of principal banding frequencies between the visual banding (Fig 4(b)) of this primary colorant and its mechanical banding (Fig 4(a)). This confirms that variations of line spacing of each primary colorant plane are a major contributor to the visual color banding. However, it is worth noting that some of the spectral lines in the mechanical banding are suppressed in the visual banding (most apparently at 18 cycles/inch); and there are low frequency spectral lines in the visual banding that are not present in the mechanical banding.

Since secondary colors are produced by superimposing a pair of corresponding primary colorants, one might expect that the overall banding from a secondary colorant plane would be an addition of those from the individual primary colorant planes. Figures 5(a), (b), and (c) show that it is not the case. As seen in these figures, some principal banding frequencies in the red visual banding spectrum are much larger than would be expected based on simple addition of the corresponding spectral components in the magenta and yellow visual banding spectra. The spectral line at 22 cycles/inch is a particular striking illustration of this phenomenon. This implies that even though individual banding from the primary colorants may be reduced below a certain visibility threshold, banding in the corresponding secondary colors may still be perceptible. We observe a similar relationship between the visual banding spectra of cyan, yellow, and green, and between the visual banding spectra of cyan, magenta, and blue.

## Conclusions

We introduced a new robust software tool for measuring principal banding frequencies exhibited by color laser printers. The tool, based on image analysis, measures banding signals from two sources: the variations of line spacing of each primary colorant, and the process-direction variations in different perceptual color attributes of both primary and secondary colorants. We also presented the banding measurement and analysis for a particular color laser printer using our developed tool. The tool is useful for printer engineers to investigate banding in color laser printers

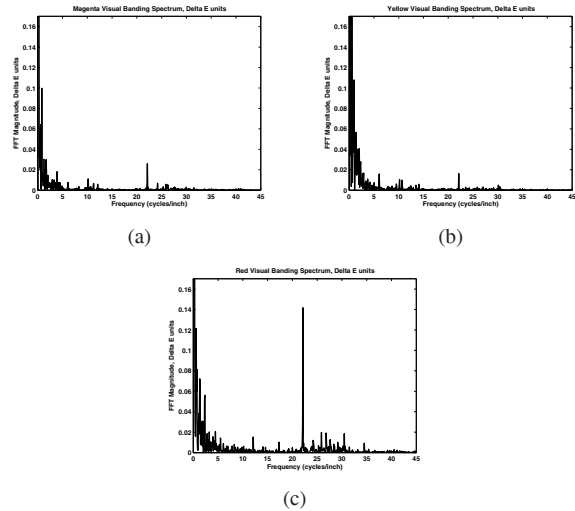


**Figure 5.** Visual banding spectrum in  $\Delta E$  units from the (a) magenta colorant plane, (b) yellow colorant plane, and (c) red colorant plane.

throughout all stages of the printer development life cycle.

## Acknowledgements

We wish to thank the Samsung Electronics Company for providing us with the opportunity to do this research.

## References

- [1] P. L. Jeran, Gear Train Control System for Reducing Velocity Induced Image Defects in Printers and Copiers, U.S. Patent 5,812,183 (1998).
- [2] W. E. Foote and R. G. Sevier, Laser Printer with Apparatus to Reduce Banding by Servo Adjustment of a Scanned Laser Beam, U.S. Patent 5,760,817 (1998).
- [3] R. P. Loce and W. L. Lama, Printer Compensated for Vibration-generated Scan Line Errors, U.S. Patent 4,884,083 (1989).
- [4] G. Y. Lin, J. Grice, J. P. Allebach, G. T. C. Chiu, W. Bradburn, and J. Weaver, Banding Artifact Reduction in Closed-loop Printing Systems by Using Pulse Width Modulation, Proc. IS&T's NIP 16, Vancouver, B.C., Canada, pg. 433-442. (2000).
- [5] Gazi N. Ali, Image Quality Analysis of Electrophotographic Printers for Banding Measurement and Forensic Application, PhD Thesis, Purdue University, 2007.
- [6] B. Min, Z. Pizlo, and J. P. Allebach, Development of Softcopy Environment for Primary Color Banding Visibility Assessment, Image Quality and System Performance V, SPIE Vol. 6808. (2008).
- [7] W. Jang and J. P. Allebach, Characterization of Printer MTF, J. of Imaging. Sci. and Tech., 50, pg. 1062-3701. (2006).
- [8] J. P. Allebach, DBS: Retrospective and Future Directions, Color Imaging: Device-Independent Color, Color Hardcopy, and Graphic Arts VI, SPIE Vol. 3963. (2000).

## Author Biography

Thanh H. Ha received his B.S in electronics from Hanoi University of Technology in 2000 and M.S in technology systems from Korea Institute of Science and Technology in 2003. Since 2005, he has been pursuing a PhD degree in the School of Electrical and Computer Engineering at Purdue University. His research interests include digital image processing and color science.